Research Article

Journal of Environmental Nanotechnology

Green Valorization of Pomegranate Peel Waste into an MgO Nanocomposite for Sustainable and High-efficiency Turbidity Removal in Water and Wastewater Treatment

A. T. Ravichandran[1], P. Rasagopal[2], G. Senthilkumar[3], J. Kumaresan[4], S. Balachandran[5] and R. Girimurugan[6]*

[1]Department of Mechanical Engineering, Vel Tech Rangarajan Dr Sagunthala R & D Institute of Science and Technology, Chennai, TN, India
[2]Department of Mechanical Engineering, K.S.R. College of Engineering, Tiruchengode, TN, India
[3]Department of Mechanical Engineering, Bannari Amman Institute of Technology, Sathyamangalam, TN, India
[4]Department of Electrical & Electronics Engineering, Nandha College of Technology, Perundurai, TN, India
[5]Department of Chemical Engineering, Vel Tech High Tech Dr. Rangarajan Dr. Sakunthala Engineering College, Chennai, TN, India
[6]Department of Mechanical Engineering, Nandha College of Technology, Perundurai, TN, India
Received: 08.07.2026 Accepted: 09.08.2026 Published: 30.09.2026
*dr.r.girimurugan@gmail.com

ABSTRACT

Pomegranate peel waste (PPW) was successfully utilized as a renewable biomass precursor to develop an MgO-based nanocomposite through a simple and environmentally sustainable synthesis process for water purification. The prepared PPW–MgO nanocomposites were systematically examined using XRD, FTIR and TGA to investigate surface functional groups, crystal structure, and thermal behavior. Among the synthesized formulations, PPW–MgO (0.50) displayed the most desirable physicochemical characteristics, with uniformly distributed MgO nanoparticles and an optimized surface charge, resulting in turbidity elimination efficiency of 81.9% under optimum coagulant dosage of 2.0 g L^{-1}, conditions of pH 4.6, and settling time of 40 min. The superior clarification efficiency was attributed to the cooperative effect of hydroxyl-rich pomegranate peel matrix and MgO NPs, which enhanced particle destabilization through interparticle bridging, sweep flocculation and charge neutralization. Relative to conventional coagulants like alum and polyaluminum chloride, PPW–MgO (0.50) achieved comparable or higher treatment performance while exhibiting excellent biodegradability, a residual Mg concentration below 0.05 mg L^{-1}, and an estimated cost of approximately ₹20 per kg. Overall, the developed MgO nanocomposite derived from pomegranate peel waste represents an economical, scalable, and environmentally sustainable material for water and wastewater treatment, while simultaneously promoting agricultural waste valorization within a circular economy framework.

Keywords: Agricultural waste; Sustainability; Biomass; Nanocomposites; Crystal structure.

1. INTRODUCTION

Wastewater generated from industrial and agricultural activities contains a wide range of organic pollutants, dyes, nutrients, and heavy metals that pose significant risks to ecosystems and human health (Kumar *et al.* 2026). Consequently, nanomaterial-based approaches have attracted increasing attention as sustainable and efficient strategies for the removal of heavy metals from wastewater (David *et al.* 2024). Various sustainable wastewater treatment approaches, including biological, physicochemical, phytoremediation, anaerobic digestion, and microbial fuel cell technologies have been extensively investigated for improving pollutant removal and promoting resource recovery (Rao *et al.* 2025). Among these approaches, pomegranate peel powder has been identified as an effective natural coagulant capable of enhancing nitrogen removal and contributing to sustainable dairy wastewater treatment (Tom, 2023). Owing to its abundance, biodegradability, porous lignocellulosic structure, and rich surface functional groups, pomegranate peel has emerged as a promising biomass precursor for the development of low-cost adsorbents. Pomegranate peel-derived powdered activated carbon has demonstrated efficient removal of BOD, COD, nitrate, and phosphate during tertiary wastewater treatment, while the addition of alum further improved pollutant removal efficiency (Al-Baidhani and Al-Khafaji, 2017).

Similarly, activated carbon prepared from pomegranate peel waste (PPW) effectively adsorbed protocatechuic acid following the Freundlich isotherm and pseudo-second-order kinetic model, highlighting its potential for sustainable wastewater remediation (Gaharwar *et al.* 2024). Crushed pomegranate peel has

also been employed as an inexpensive biosorbent for mercury and cadmium removal, achieving maximum adsorption capacities of 42.13 mg/g and 89.59 mg/g, respectively, according to the Langmuir isotherm model (Zareei *et al.* 2024). Furthermore, pomegranate peel exhibited excellent adsorption performance for Brilliant Blue R and Victoria Blue R dyes, attaining removal efficiencies of 90.38% and 100%, respectively (Akmese, 2025).

To further improve adsorption efficiency, numerous modified pomegranate peel-based materials have been developed. A kaolinite-modified pomegranate peel hydrochar composite demonstrated enhanced Malachite Green adsorption with improved structural stability while following Langmuir isotherm and pseudo-second-order kinetic behavior (Azizi and Alorabi, 2025). Iron(III)-loaded pomegranate peel powder significantly enhanced phosphate removal, achieving a maximum adsorption capacity of 99.30 mg/g (Bashyal *et al.* 2023). Microwave-assisted nitrogen doping increased the surface area and functional groups of pomegranate peel-derived biochar, resulting in superior Cd(II) adsorption performance (Murat *et al.* 2025). Likewise, phosphoric acid-activated pomegranate peel waste produced highly porous activated carbon capable of removing 89.36% of Brilliant Blue dye under optimized conditions (Al-Hussainy *et al.* 2025). Activated carbon impregnated with nanoscale zero-valent iron further enhanced furfural adsorption, achieving a maximum adsorption capacity of 222.22 mg/g (Rashtbari *et al.* 2022).

The incorporation of functional nanomaterials into pomegranate peel matrices has further expanded their wastewater treatment applications. A pomegranate peel powder/reduced graphene oxide nanocomposite exhibited high adsorption capacities for the simultaneous removal of Pb(II) ions and Methylene Blue while maintaining excellent stability and reusability (Hassan *et al.* 2025). Novel pomegranate peel-based nanocomposites incorporating chitosan, *Padina pavonica*, Fe(III), and nano-MgO demonstrated efficient removal of Cu(II) and Cd(II), with the MgO-modified composite exhibiting the highest adsorption performance and excellent regeneration ability (Hamad and Ibrahim. 2024). In addition, pomegranate skin proved to be an effective green adsorbent for Yellow Bemacid dye removal by following the Langmuir isotherm and pseudo-second-order kinetic model (Henini *et al.* 2024). Beyond adsorption, nutrient-fortified pomegranate peel powders have also been investigated as sustainable bioadsorbent-derived biofertilizers, where nutrient enrichment reduced phytotoxicity and enhanced plant growth, demonstrating the broader environmental applications of pomegranate peel biomass (Bodor *et al.* 2024).

In recent years, MgO nanoparticles have attracted considerable attention as visible-light-responsive photocatalysts because of their high chemical stability, low toxicity, and strong oxidative capability. Green-synthesized MgO nanoparticles achieved more than 95% degradation of Rhodamine B and Methylene Blue dyes under visible-light irradiation, demonstrating excellent photocatalytic performance (Pachiyappan *et al.* 2022). Oxygen-vacancy-rich MgO nanoparticles synthesized using lemon peel extract exhibited enhanced Crystal Violet degradation owing to improved charge separation and abundant active sites (Tamam *et al.* 2025). Similarly, Cu-doped MgO nanoparticles showed superior photocatalytic degradation of Methylene Blue through band-gap reduction and improved sunlight utilization (Arif *et al.* 2022).

To combine adsorption and photocatalysis within a single material, several hybrid nanocomposites have recently been developed. Green-synthesized rGO/MgO nanocomposites achieved approximately 93% degradation of Methylene Blue under solar irradiation while simultaneously exhibiting strong antibacterial activity (Abel *et al.* 2025). A MnO_2/diosgenin–chitosan nanocomposite demonstrated efficient visible-light degradation of Acid Green and Malachite Green Oxalate dyes together with excellent antimicrobial properties (Raj *et al.* 2025). Magnetic graphene oxide functioned as a recyclable adsorbent for Methylene Blue removal, exhibiting a maximum adsorption capacity of 78.13 mg/g while maintaining more than 90% removal efficiency after repeated use (Jalali *et al.* 2019). Furthermore, green-synthesized nanoparticles derived from pomegranate peel, moringa seed waste, and sawdust were successfully employed for the removal of Cr(VI) from contaminated water, achieving removal efficiencies of 96–100% under column conditions and demonstrating the effectiveness of agricultural waste-derived nano-biosorbents for heavy metal remediation (Mahdy and Fathi, 2026). Building upon the utilization of pomegranate peel as a green precursor for nanomaterial synthesis, pomegranate peel extract was further employed to synthesize CuO nanoparticles, which exhibited outstanding photocatalytic degradation efficiencies of 98% for Methylene Blue and 95% for methyl orange while maintaining excellent stability over repeated reuse cycles (Arif *et al.* 2024).

Pomegranate peel waste is an abundant agricultural residue that remains largely underutilized despite its high content of carboxyl- and hydroxyl-containing functional groups, which provide favorable active sites for surface modification and the immobilization of metal oxide nanoparticles. Utilizing this biomass as a precursor for MgO-based bio-nanocomposites represents an environmentally sustainable strategy that supports the concepts of circular

bioeconomy and the green chemistry. This value-added conversion transforms discarded agro-waste into functional material suitable for water purification uses. Nanocomposites exhibit enhanced surface activity, improved coagulation performance, and reduced environmental load, making them promising candidates for practical water and wastewater treatment. The novelty of the present work lies in the development of pomegranate peel waste-derived MgO bio-nanocomposites as sustainable coagulation materials, an area that has received limited scientific attention. Although biomass-derived adsorbents and coagulants have been widely investigated, the fabrication of hybrid MgO nanocomposites from PPW for coagulation–flocculation applications remain largely unexplored. Therefore, this study expands the scope of agricultural biomass valorization while presenting an innovative route for producing efficient, environmentally benign materials for water purification.

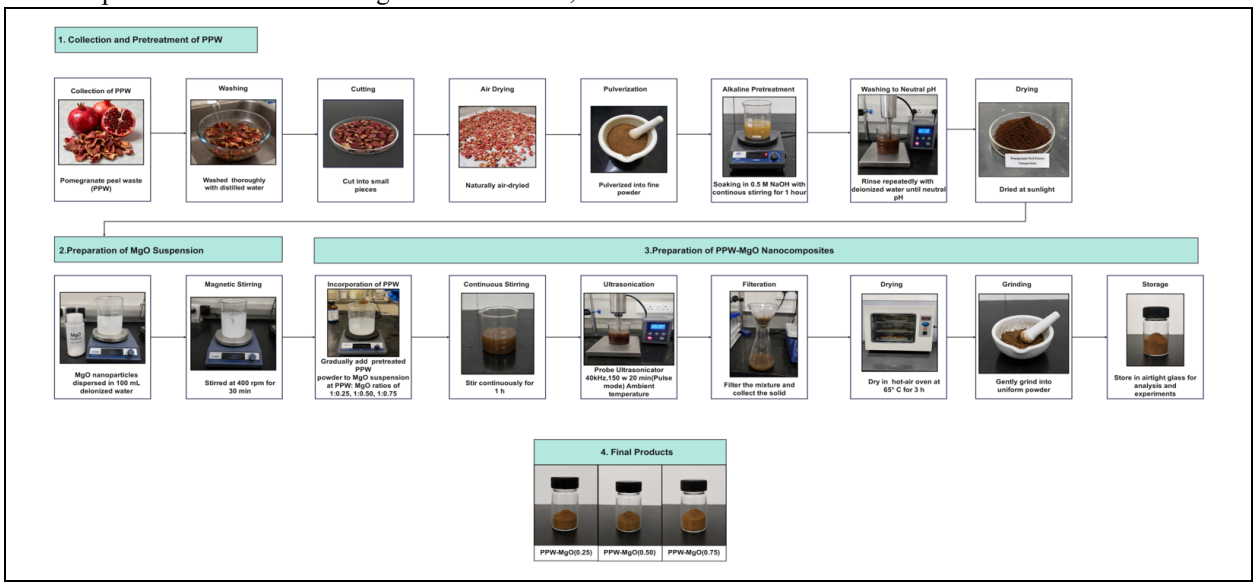

Fig. 1: Preparation process of MgO-based nanocomposites

2. MATERIALS AND METHODS

2.1 Materials

Fresh pomegranate peel waste was collected from a local fruit market. Analytical-grade reagents, including sodium hydroxide (NaOH, ≥98% purity), magnesium oxide (MgO, ≥99% purity), kaolin (≥99% purity), and sulfuric acid (98% purity) were obtained from Sigma-Aldric. Deionized water served as solvent for all solution preparation and experimental procedures to minimize contamination. Solution pH was monitored by Adwa AD11 pH meter, whereas turbidity measurements were performed with HACH TL2300 turbidimeter. Coagulation–flocculation experiments were conducted using conventional jar test method with six-position programmable jar test unit fitted with 6 variable-speed mixing and one-liter beakers.

2.2 Nanocomposite Preparation Process

Pomegranate peel waste was collected, washed thoroughly with distilled water to remove adhering impurities, and cut into small pieces before being naturally air-dried. The dried material was pulverized into a fine powder and subjected to alkaline pretreatment by soaking in 0.5 M NaOH with continuous stirring for 1 hour. Pomegranate peel powder was prepared with modifications based on the preprocessing approach reported by (Abinaya *et al.* 2024). After treatment, the powder was repeatedly rinsed with deionized water until the wash solution reached neutral pH and then dried in sunlight. For the preparation of MgO-based nanocomposites, analytical-grade MgO nanoparticles were dispersed in 100 mL of deionized water and magnetically stirred at 400 rpm for 30 min to obtain a uniform suspension. Green synthesis of magnesium oxide nanoparticles (MgO NPs) was carried out using the same method as reported by (Kalidasan *et al.* 2026). The pretreated PPW powder were gradually incorporated into MgO dispersion at PPW:MgO ratios of 1:0.25, 1:0.50, and 1:0.75. Continuous stirring was maintained for an additional 1 hour to promote effective interaction between the biomass matrix and MgO nanoparticles. To improve particle dispersion and suppress agglomeration, the suspensions were further treated using a probe ultrasonicator operated at 40 kHz and 150 W for 20 minutes in pulse mode at ambient temperature. The resulting mixture was filtered, and recovered solid was dried in a hot-air oven at 65 °C for 3 hours. Dried products were gently ground into a uniform powder and preserved in airtight glass for physicochemical

characterization and coagulation–flocculation experiments. Synthesized nanocomposites were designated as PPW–MgO (0.25), PPW–MgO (0.50), and PPW–MgO (0.75), corresponding to MgO loadings of 0.25, 0.50, and 0.75 g/g of PPW, respectively. The overall recovery yield after drying remained within 87–92%, indicating that the synthesis procedure (Fig. 1) involved minimal material loss.

Table 1. Characteristics of synthetic wastewater

Property	Observed Value	Measurement Technique
Water medium	Tap water	–
Initial turbidity	576 ± 5	HACH TL2300 turbidimeter
Kaolin quality	≥99	Manufacturer specification
Kaolin loading	1.0	Analytical balance
Agitation speed	400	Bio Tron magnetic stirrer
Agitation period	30	Stopwatch
Preparation temperature	30 ± 2	Laboratory ambient conditions
Suspension pH	7.2 ± 0.1	Calibrated digital pH meter
Dissolved solids	145 ± 10	Conductivity/TDS meter
Electrical conductivity	225 ± 10	Conductivity meter
Physical appearance	Homogeneous colloidal dispersion	Visual inspection

2.3 Preparation of Synthetic Wastewater

The wastewater was prepared for coagulation–flocculation studies using kaolin as the suspended particulate material. Briefly, 10 g of kaolin powder was added to 10 L of tap water at ambient temperature to prepare stock suspension. The mixture was initially blended manually to disperse the particles, followed by continuous stirring at 400 rpm for 30 minutes to obtain a homogeneous suspension. Subsequently, the suspension was allowed to stand overnight to ensure hydration of kaolin particles and stabilization of the colloidal system. The resulting synthetic wastewater showed initial turbidity of 576 NTU and was used as the stock solution throughout investigation. The physicochemical properties of prepared turbid water are summarized in Table 1.

Experimental suspensions with the desired turbidity values were prepared by diluting the stock suspension to the required concentrations before each coagulation–flocculation experiment, as summarized in Table 2.

Table 2. Surface charge characteristics of PPW-based materials

pH	PPW	PPW-NaOH	PPW-MgO (0.25)	PPW-MgO (0.50)	PPW-MgO (0.75)
2	+5	+2	+15	+20	+25
4	-2	-10	+5	+10	+15
6	-15	-30	-5	+2	+8
7	-20	-38	-12	-6	+1
8	-28	-45	-22	-18	-10
10	-35	-55	-30	-28	-20

2.4 Characterization

2.4.1 Surface Charge Analysis

The surface charge behavior of raw PPW, alkali-treated PPW (PPW–NaOH), and the synthesized PPW–MgO nanocomposites was determined by zeta potential analysis (Gemini, Zeiss). The analysis was performed to investigate electrokinetic characteristics of prepared materials and to assess effect of alkali treatment and MgO incorporation on their surface properties. Variations in zeta potential reflected changes in surface charge resulting from chemical modification and nanocomposite formation, which directly influenced particle stability, aggregation behavior, and dispersion characteristics. The obtained results provide a better understanding of the interfacial interactions responsible for the improved coagulation efficiency and water purification performance of the developed nanocomposites.

2.4.2 FTIR Analysis

Chemical characteristics of prepared specimens were examined by Fourier Transform Infrared Spectroscopy to identify surface functional groups responsible for coagulation behavior. The spectra were recorded on a Bruker instrument in the wavenumber region 4000–400 cm^{-1} at a spectral resolution of 1 cm^{-1}.

2.4.3 XRD Analysis

The phase composition and crystalline structure of the prepared samples was examined using Powder X-ray Diffraction (XRD). Data collection was performed over a 2θ range of 5–80° using a step interval of 0.02° and a scanning speed of 1–2° min^{-1}. Before analysis, each sample was finely ground, uniformly spread onto a glass sample holder, and the instrument was calibrated with a silicon reference standard to ensure measurement reliability. The recorded diffractograms were matched with ICDD standard patterns to identify crystalline phases and assess degree of crystallinity. These structural characteristics were subsequently correlated with the coagulation behavior and turbidity removal efficiency of the developed materials.

2.4.4 TGA Analysis

The thermal behavior and stability of the prepared materials were investigated using Thermogravimetric Analysis (TGA Q50 analyzer). For each measurement, 5–10 mg of sample was loaded into platinum crucible and heated from ambient temperature to 800–1000°C at uniform rate of 10 °C min^{-1} at continuous nitrogen flow to minimize oxidative degradation. The TGA curves were analyzed to identify the successive mass-loss regions corresponding to moisture removal, decomposition of organic constituents, and structural transformations occurring during heating. The obtained thermal characteristics were further used to assess the stability of the synthesized materials and their relevance to coagulation performance.

2.5 Optimization of Coagulation Parameter

A systematic set of coagulation–flocculation was performed to optimize operating conditions and evaluate treatment efficiency of synthesized PPW–MgO nanocomposites. The effect of solution pH was initially investigated over the range 4.4 – 8.5, covering the conditions commonly encountered in wastewater and natural water treatment processes. The desired pH values were adjusted by 0.50 M H_2SO_4 and 0.50 M NaOH solutions, while a calibrated digital pH meter was employed to monitor and confirm the pH throughout the experiments, ensuring reliable and accurate measurements.

The influence of coagulant dosage was assessed by adjusting the concentration of the synthesized PPW–MgO nanocomposites from 0.4 to 2.6 g L^{-1}. To study the effect of the initial turbidity, synthetic water samples containing kaolin concentrations between 0.5 and 4.0 g L^{-1} were prepared. Settling behavior was evaluated by collecting clarified supernatant after 20 – 100 minutes. The PPW–MgO nanocomposites were used at wet state, and coagulation–flocculation experiments were carried out under standardized operating conditions consisting of rapid agitation at 250 rpm for 5 minutes, followed by gentle mix at 50 rpm for 10 minutes. Every experiment was repeated three times, and the reported results represent reproducible measurements with acceptable statistical reliability.

2.5.1 Jar Test Procedure

Coagulation–flocculation experiments were performed using the conventional jar test protocol. The jar test unit consisted of 6 one-L beakers, all containing synthetic turbid water with initial turbidity of 576 NTU otherwise indicated. Before adding PPW–MgO nanocomposite coagulants, the initial pH of every suspension was recorded. The required coagulant dosage was then added, followed by stirring at 250 rpm for 5 minutes and slow agitation at 50 rpm for 5 minutes to promote floc formation. The suspensions were subsequently left undisturbed for 40 minutes to allow sedimentation of the formed flocs. After the settling period, the clarified supernatant was carefully withdrawn for turbidity analysis. The percentage of turbidity removal was determined according to Eq. (1).

$$\text{Efficiency } \% = \frac{\text{Initial turbidity} - \text{Final turbidity}}{\text{Initial turbidity}} \times 100 \quad \ldots (1)$$

3. RESULTS AND DISCUSSION

3.1 Surface Charge Characteristics

The profiles of raw pomegranate peel waste (PPW), alkali-treated PPW (PPW–NaOH), and the synthesized PPW–MgO nanocomposites (PPW–MgO (0.25), PPW–MgO (0.50), and PPW–MgO (0.75)) reveal distinct variations in surface charge that govern colloidal stability and interfacial interactions. Following alkali treatment, PPW–NaOH displayed a substantially more negative zeta potential across the investigated pH range, indicating enhanced exposure of ionizable oxygen-containing functional groups after partial removal of surface impurities and non-cellulosic constituents. In contrast, incorporation of MgO nanoparticles progressively shifted the surface charge toward less negative values, particularly under acidic and near-neutral conditions. The PPW–MgO (0.25) nanocomposite exhibited only a slight reduction in negative surface charge, whereas PPW–MgO (0.50) and PPW–MgO (0.75) maintained near-neutral or weakly positive zeta potentials over a broader pH range, demonstrating the increasing contribution of MgO to the overall surface characteristics. This behavior can be attributed to the amphoteric nature of surface Mg–OH groups, which become protonated under acidic conditions and gradually deprotonate with increasing pH, thereby shifting the apparent isoelectric point of the nanocomposites. Consequently, PPW–NaOH showed superior electrostatic stability at alkaline pH because of its highly negative surface charge, while the MgO-containing composites exhibited lower absolute zeta

potential values around neutral pH, promoting particle aggregation and improving charge neutralization during coagulation. These findings confirm that alkali treatment primarily enhances the density of negatively charged functional groups on the biomass surface, whereas MgO incorporation modifies the electrokinetic behavior by introducing amphoteric surface sites. Such tunable surface-charge characteristics are advantageous for improving coagulation efficiency, pollutant interaction, and suspension behavior under different water treatment conditions.

3.2 FTIR Characteristics

Fig. 2 presents the FTIR spectra of raw PPW, PPW–NaOH, and PPW–MgO nanocomposites containing MgO loadings of 0.25, 0.50, and 0.75. Comparison of the spectra demonstrates noticeable changes in the chemical structure of the lignocellulosic biomass after alkali treatment and confirms the establishment of interfacial interactions between MgO nanoparticles and the pomegranate peel matrix during nanocomposite formation.

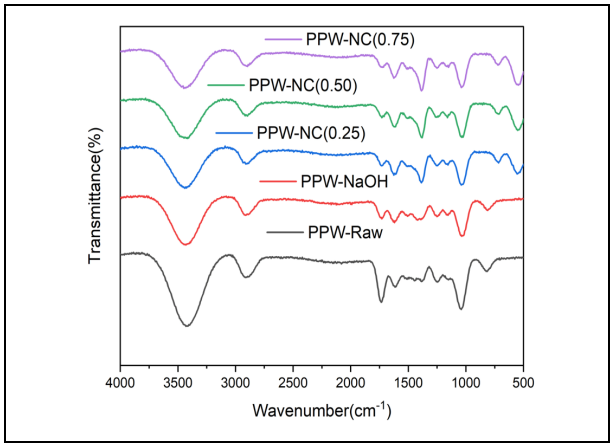

Fig. 2: Functional group analysis of raw pomegranate peel waste

The FTIR spectrum of raw PPW exhibits broad peak centered at 3435 cm^{-1} attributed to stretching vibration of hydroxyl groups originating from hemicellulose, cellulose and physically adsorbed moisture. Following alkaline treatment, intensity of this peak increases in PPW–NaOH, indicating greater exposure of hydroxyl-containing functional groups due to the partial elimination of hemicellulosic and lignin constituents. Peaks observed in the 2915 cm^{-1} region correspond to symmetric and asymmetric stretching vibrations of aliphatic C–H bonds present in lignocellulosic framework. A distinct peak near 1725 cm^{-1}, assigned to carbonyl stretching vibration of ester groups associated with hemicellulose and lignin, becomes considerably weaker after alkali treatment and further diminishes with increasing MgO incorporation, confirming the cleavage of ester linkages and removal of non-cellulosic components. The absorption region between 1605 and 1630 cm^{-1} is mainly related to the bending vibration of adsorbed water together with residual aromatic structures from lignin. After incorporation of MgO nanoparticles, additional bands together with enhanced absorption intensity are observed within the 650–520 cm^{-1} region, which are attributed to Mg–O stretching vibrations and Mg–O–C interfacial interactions, demonstrating successful immobilization of MgO onto the biomass surface. Increasing the MgO loading from PPW–MgO (0.25) to PPW–MgO (0.75) produces gradual peak shifts and improved spectral definition, indicating stronger interactions between the inorganic phase and the lignocellulosic matrix as well as the formation of bio-nanocomposite structure. According to earlier studies, FTIR analysis confirmed the successful incorporation of cellulose extracted from pomegranate peel waste and chemically crosslinked chitosan through hydrogen bonding within the composite structure. The identified functional groups verified the formation of a stable bio-based adsorbent with abundant active sites for efficient Methyl Orange adsorption (Fadhil *et al.* 2026). Overall, the FTIR results verify effective chemical modification of pomegranate peel waste and uniform incorporation of MgO nanoparticles, which are expected to improve the surface functionality and coagulation performance of the developed nanocomposites.

3.3 XRD Characterization

Fig. 3 presents the XRD patterns of raw and alkali-treated pomegranate peel waste together with the synthesized PPW–MgO nanocomposites, illustrating the structural changes induced by chemical pretreatment and MgO incorporation.

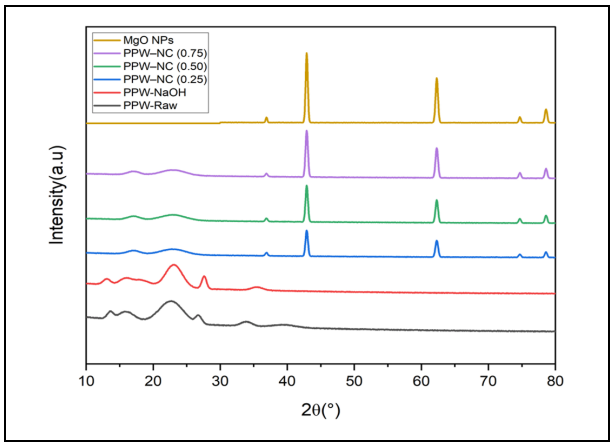

Fig. 3: XRD patterns of PPW samples

The XRD pattern of raw PPW is characterized by a broad diffraction band within the 2θ range of approximately 15–25°, indicating the predominantly amorphous nature of the lignocellulosic biomass with only limited crystalline ordering. After alkaline

pretreatment, the diffraction feature of PPW–NaOH becomes relatively sharper, suggesting partial elimination of amorphous hemicellulose and lignin, which improves structural organization of the cellulose phase. In comparison, MgO exhibits distinct crystalline reflections at approximately 2θ = 36.8°, 42.9°, 62.3°, 74.8°, and 78.7°, corresponding to (111), (200), (220), (311), and (222) planes of the cubic periclase structure, confirming its high crystallinity. The diffraction profiles of the PPW–MgO nanocomposites reveal the gradual appearance and increased intensity of these characteristic MgO peaks with increasing MgO loading from PPW–MgO (0.25) to PPW–MgO (0.75), demonstrating successful addition of crystalline MgO into biomass matrix. Simultaneously, broad amorphous halo associated with pomegranate peel waste becomes less prominent, indicating effective deposition of MgO nanoparticles on the lignocellulosic framework. The enhanced peak intensity observed for PPW–MgO (0.75) reflects improved crystallinity and stronger interaction between the MgO phase and oxygen functional groups of biomasses. Overall, XRD outcomes verify successful formation of PPW–MgO bio-nanocomposites, in which crystalline MgO is uniformly integrated with the lignocellulosic support, contributing to enhanced structural stability, surface activity, and coagulation performance. Benahdach *et al.* (2025) performed XRD analysis to confirm the successful formation of activated carbon derived from pomegranate peel waste (PPW-derived AC) with a predominantly amorphous carbon structure suitable for adsorption. The structural characteristics verified by XRD supported the effective adsorption of Congo Red dye from wastewater.

3.4 TGA Characterization

The thermogravimetric profiles of PPW exhibit a characteristic multistage degradation behavior typical of lignocellulosic biomass. As illustrated in Fig. 4, the initial weight-loss region (<100°C) is primarily attributed to evaporation of adsorbed moisture and other volatile constituents present on the material surface.

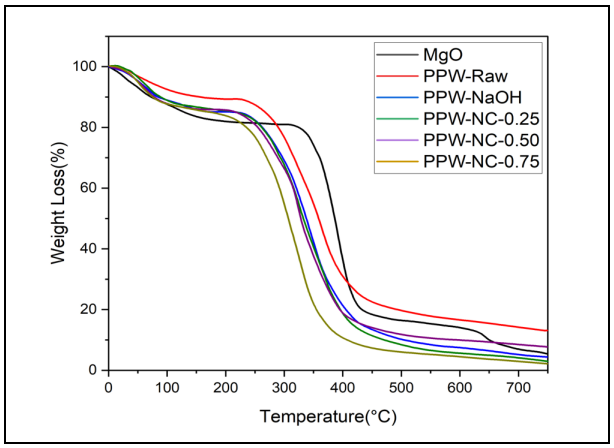

Fig. 4: TGA profiles of PPW samples

A pronounced mass-loss stage is observed between 250 and 420 °C, corresponding mainly to thermal decomposition of cellulose and hemicellulose fractions present in pomegranate peel waste matrix. Beyond 420°C, weight decreases gradually because of the progressive degradation of the thermally stable lignin component. Among all the investigated samples, raw PPW shows the greatest residual mass owing to the presence of undecomposed inorganic constituents and carbonaceous residues. In comparison, PPW–NaOH and the PPW–MgO nanocomposites exhibit improved thermal resistance, as evidenced by the delayed onset of decomposition and higher residual mass at the end of the analysis (600–730 °C). The enhancement in thermal stability becomes more pronounced with increasing MgO loading, indicating effective interfacial interactions between the lignocellulosic matrix and MgO nanoparticles, which restrict polymer chain mobility and retard thermal degradation. These thermogravimetric results confirm that alkali pretreatment together with MgO incorporation significantly improves the thermal stability of pomegranate peel waste, highlighting its suitability as a durable biomass-based material for coagulation and environmental remediation applications. Kamalesh and Saravanan, (2026) have confirmed the excellent thermal stability of the raw pomegranate peel waste-loaded ZIF-8 (RPZIF-8) adsorbent, with the Zn–N framework remaining structurally intact during thermal treatment by TGA. The results demonstrated that RPZIF-8 possesses sufficient thermal robustness for repeated adsorption–regeneration cycles in wastewater treatment applications.

3.5 Coagulation Performance of PPW−MgO

3.5.1 Influence of pH

Fig. 5 presents the influence of solution pH on turbidity elimination efficiency (R%) of the PPW–MgO nanocomposites containing MgO loadings of 0.25, 0.50, and 0.75. Regardless of the MgO content, all nanocomposites exhibited a similar bell-shaped response, demonstrating that the coagulation efficiency was strongly governed by the solution pH.

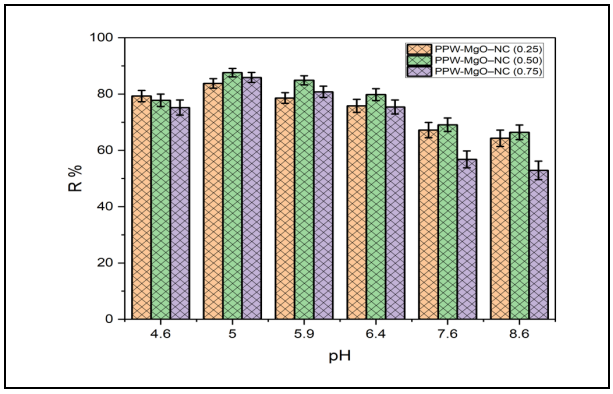

Fig. 5: pH-dependent coagulation efficiency

Turbidity removal efficiency improved progressively as the solution pH shifted from alkaline to mildly acidic, reaching the highest value at approximately pH 5.0. Among the investigated formulations, PPW–MgO (0.50) achieved the maximum removal efficiency of nearly 87.6%, indicating that this composition provided the most favorable combination of surface charge characteristics and homogeneous MgO nanoparticle distribution for efficient particle destabilization and adsorption. In comparison, PPW–MgO (0.75) exhibited a slight reduction in performance, particularly under alkaline conditions, which may be associated with partial nanoparticle agglomeration and a decrease in number of accessible active sites. As pH increased beyond 7, the removal efficiency of all nanocomposites gradually decreased because of reduced protonation of weaker electrostatic interactions and surface functional groups with suspended colloidal particles. These findings demonstrate that mildly acidic conditions provide the most suitable environment for coagulation, with PPW–MgO (0.50) exhibiting the optimum balance between coagulation efficiency and structural stability.

3.5.2 Dosage Effect

Fig. 6 shows the effect of coagulant dosage on turbidity elimination efficiency of the synthesized PPW–MgO nanocomposites containing MgO loadings of 0.25, 0.50, and 0.75. The coagulation performance of the three formulations was evaluated over the investigated dosage range to determine the optimum operating condition.

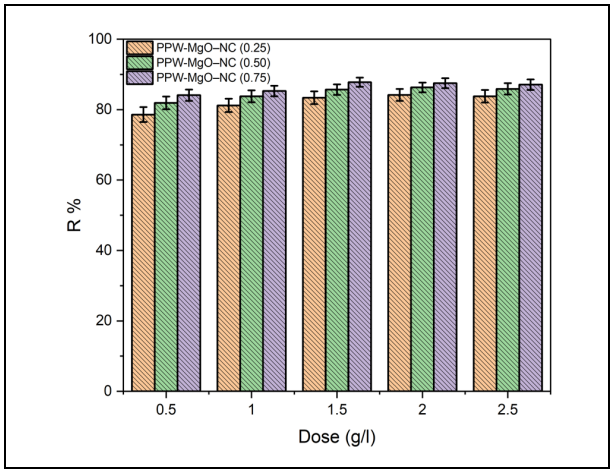

Fig. 6: Dosage-dependent coagulation performance

Coagulant dosage increased, turbidity removal efficiency of all PPW–MgO nanocomposites improved steadily until reaching 2.0 g L^{-1}, beyond which only marginal changes were observed, indicating the optimum dosage had been achieved. Among the prepared formulations, PPW–MgO (0.50) produced the highest removal efficiency (≈81.9%), demonstrating that this composition provided the most favorable balance between MgO nanoparticle dispersion and the availability of active coagulation sites. By comparison, PPW–MgO (0.75) exhibited a slightly lower removal efficiency, which may be attributed to partial nanoparticle agglomeration at higher MgO loading, reducing the accessibility of reactive surface sites. The negligible improvement observed above 0.5–2.0 g L^{-1} indicates that additional coagulant does not significantly enhance particle destabilization because most suspended colloids have already been removed, while excess dosage may increase the concentration of residual solids. These observations demonstrate that both the MgO loading and the applied coagulant dosage play critical roles in achieving maximum turbidity removal efficiency, with PPW–MgO (0.50) representing the optimum formulation.

3.5.3 Effect of Initial Concentration

Fig. 7 illustrates effect of the initial turbidity concentration on removal efficiency (R%) of the synthesized PPW–MgO nanocomposites containing MgO loadings of 0.25, 0.50, and 0.75. The coagulation performance of each formulation was evaluated over different initial contaminant concentrations to assess its treatment capability under varying turbidity conditions.

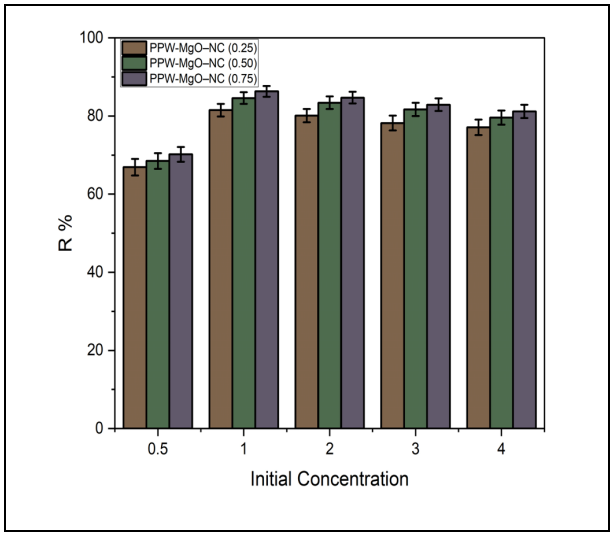

Fig. 7: Turbidity-dependent coagulation performance

The turbidity removal efficiency raised rapidly as initial contaminant concentration increased 0.5 to 2.0 g L^{-1}, after which the values stabilized within the range of approximately 84–87%. This trend indicates that sufficient active coagulation sites were initially available on the PPW–MgO nanocomposites, enabling efficient particle destabilization through adsorption, charge neutralization, and floc formation. As the contaminant concentration increased further, the available surface sites gradually approached saturation, resulting in only minor changes in removal efficiency. Among the investigated formulations, PPW–MgO (0.50)

consistently achieved the highest turbidity removal over the entire concentration range, suggesting that this composition provided the optimum distribution of MgO nanoparticles and the greatest number of accessible reactive sites. In comparison, PPW–MgO (0.75) exhibited a slight decrease in performance at higher contaminant concentrations, which may be attributed to partial MgO nanoparticle agglomeration that reduced the effective surface area available for coagulation. The comparatively lower efficiency of PPW–MgO (0.25) was associated with its lower MgO content, resulting in fewer active sites for contaminant removal. Overall, the PPW–MgO nanocomposites, particularly PPW–MgO (0.50) maintained a consistently high turbidity removal efficiency of approximately 86.3% over a broad concentration range, demonstrating excellent operational stability and strong potential.

3.5.4 Effect of Settling Time

Fig. 8 depicts effect of settling time on the turbidity removal efficiency (R%) of the synthesized PPW–MgO nanocomposites containing MgO loadings of 0.25, 0.50, and 0.75. The settling behavior of each formulation was evaluated over different sedimentation periods to determine the optimum settling time for effective coagulation.

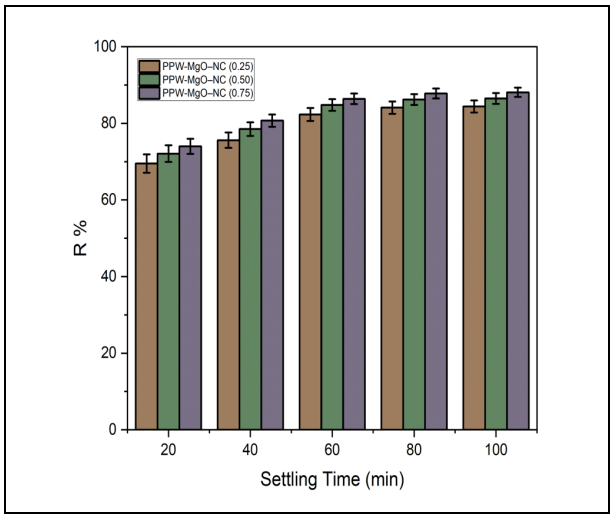

Fig. 8: Time-dependent turbidity removal

The turbidity removal efficiency gradually increased with increasing settling time, with the most significant improvement occurring during the initial 60 minutes, after which only slight changes were observed, indicating that the coagulation process had approached equilibrium. This trend is characteristic of coagulation–flocculation, where small flocs generated during rapid mixing progressively combine into denser and larger aggregates that settle efficiently under gravity. Among the formulations, PPW–MgO (0.50) consistently achieved the highest clarification efficiency, reaching 84.2–87.7% after 100 minutes, whereas PPW–MgO (0.75) and PPW–MgO (0.25) exhibited comparatively lower removal efficiencies. The enhanced performance of PPW–MgO (0.50) is attributed to the optimum MgO loading, which provides a favorable balance between available active sites and uniform nanoparticle dispersion, thereby improving adsorption, charge neutralization, and floc formation. In contrast, the slightly lower efficiency of PPW–MgO (0.75) may be associated with partial MgO nanoparticle agglomeration at higher loading, resulting in reduced effective surface area. The continuous increase in turbidity removal with settling time confirms that prolonged sedimentation enhances the separation of suspended particles from the treated water. The nearly constant removal efficiency observed after 60–80 minutes further indicates that floc growth and sedimentation had essentially reached completion, and extending the settling period produced only limited additional improvement. In a previous study, pomegranate seed powder demonstrated effective coagulation–flocculation performance for pulp and paper wastewater treatment, with enhanced efficiency when combined with alum. The dual-flocculation system achieved 81% COD removal and 98% turbidity removal through synergistic coagulation and bridging mechanisms (Shabanizadeh and Taghavijeloudar, 2023b).

3.6. Flocculation Dynamics Analysis

The coagulation kinetics of the PPW–MgO nanocomposites demonstrate a rapid multistep flocculation process, in which suspended particles are initially destabilized during the rapid mixing stage, followed by progressive floc growth, consolidation, and sedimentation under gentle mixing and settling conditions. Using the applied operating procedure, charge neutralization and the formation of primary microflocs occurred during the initial mixing stage, whereas subsequent particle collisions promoted floc enlargement through adsorption, interparticle bridging, and sweep flocculation. Accordingly, the greatest improvement in turbidity elimination was observed within first 20–60 minutes of settling. Among investigated formulations, PPW–MgO (0.50) reached near-equilibrium performance after approximately 60–80 minutes, with only minor increases in removal efficiency thereafter, indicating the formation of compact and rapidly settling flocs. The lower MgO loading provided fewer effective coagulation sites, whereas excessive MgO content promoted partial nanoparticle agglomeration, both of which reduced floc growth and settling efficiency. Overall, the time-dependent removal profiles and optimized mixing conditions confirm that PPW–MgO nanocomposites exhibit favorable coagulation kinetics for practical water treatment, achieving efficient clarification within a relatively short operating period through the combined effects of rapid charge neutralization, effective floc growth, and accelerated sedimentation. Previous studies have

reported that, the natural bio-coagulants, including moringa leaves, chitosan, opuntia, pomegranate peel, lupin straw, sugarcane bagasse, and tea waste residue, promoted flocculation by aggregating pollutants into larger, settleable flocs. An optimum dosage of 0.8g/L achieved efficient removal of turbidity, suspended solids, organic matter, and nutrient contaminants (Ahmed *et al.* 2024).

3.7 Comparative Coagulation Performance

Under the optimized operating conditions, the PPW–MgO (0.50) nanocomposite reached turbidity removal efficiency of 81.9%. This performance is higher than that reported for many conventional alum-based coagulants, for which turbidity removal efficiencies generally range from approximately 50–85% depending on the water characteristics, operating conditions, and applied dosage. These findings demonstrate that the developed PPW–MgO nanocomposites provide coagulation performance comparable to widely used pre-hydrolyzed aluminum coagulants while offering additional environmental benefits associated with the utilization of pomegranate peel waste as a renewable biomass support and the reduced risk of residual inorganic contaminants. Shabanizadeh and Taghavijeloudar, (2023a) employed pomegranate seed powder as a natural coagulant, promoting particle destabilization through charge neutralization by increasing the zeta potential of wastewater to the isoelectric point. Under optimum conditions (2391.91 mg/L, pH 10.37, 25 minutes), it achieved 98% turbidity and 87% COD removal.

3.8 Residual Mg Analysis

The concentration of residual magnesium remaining in the treated water after coagulation with PPW–MgO (0.50) was lower than 0.05 mg L^{-1}, quantified by ICP–OES following a validated sample digestion protocol and instrumental analysis with limits substantially lower than the measured concentration. The negligible residual Mg concentration indicates that the synthesized nanocomposite remained highly stable during the coagulation process, with minimal release of Mg species into the treated water. Although World Health Organization has not established a health-based guideline value specifically for magnesium in drinking water, the measured residual concentration is considerably lower than levels generally regarded as acceptable in drinking water. These observations demonstrate that the developed PPW–MgO nanocomposite not only provides efficient turbidity removal but also maintains a favorable environmental safety profile by minimizing magnesium release under the investigated operating conditions.

3.9 Economic Feasibility Analysis

A comparative economic assessment was performed to examine the cost-effectiveness of the developed PPW–MgO nanocomposites for water treatment applications. The estimated production cost of the optimized PPW–MgO (0.50) nanocomposite is approximately ₹20 per kg, mainly because pomegranate peel waste is an inexpensive and readily available biomass, while only a moderate amount of MgO is required during synthesis. By comparison, the market price of commonly used polyaluminum chloride is approximately ₹45–48 per kg, whereas commercial chemical coagulants are generally available within a broader price range of ₹2–52 per kg, depending on their composition and intended application. Although the overall treatment cost may vary with operating conditions, dosage, and raw water quality, the developed PPW–MgO nanocomposite offers a cost-effective alternative without compromising treatment efficiency. Combined with high turbidity elimination efficiency (≈86.4%) and a residual magnesium concentration below 0.05 mg L^{-1}, PPW–MgO nanocomposite represents an environmentally sustainable, economically attractive, and practical substitute for wastewater treatment.

3.10 Elucidation of Removal Mechanism

The excellent turbidity removal performance of the PPW–MgO nanocomposites is attributed to the combined contribution of several complementary coagulation mechanisms governed by their surface chemistry, microstructure, and pH-dependent electrokinetic properties. Under the optimum operating conditions (pH 4.6 and a coagulant dosage of approximately 2.0 g L^{-1}), PPW–MgO (0.50) exhibited the highest clarification efficiency (≈84–87%) because this formulation provided the most favorable balance between MgO nanoparticle distribution and surface charge characteristics. Zeta potential analysis demonstrated that MgO incorporation gradually modified the highly negative surface of alkali-treated PPW toward a less negative or near-neutral electrokinetic state, thereby enhancing charge neutralization and electrostatic attraction of suspended colloidal particles under mildly acidic conditions. At the same time, the abundant carboxyl and hydroxyl functional groups present on pomegranate peel matrix supplied numerous sites, while the lignocellulosic framework promoted interparticle bridging, resulting in the formation of larger and more stable flocs. The FTIR analysis confirmed the interaction between MgO nanoparticles and oxygen-containing functional groups of the biomass, while XRD results further verified the successful incorporation of crystalline MgO into the lignocellulosic matrix. In contrast, excessive MgO loading in PPW–MgO (0.75) resulted in partial nanoparticle agglomeration, reducing the availability of active coagulation sites and limiting treatment efficiency. The coagulation process followed a

typical sequence involving rapid particle destabilization during high-speed mixing, subsequent floc growth through adsorption, bridging, charge neutralization, and sweep flocculation during slow mixing, and efficient sedimentation within approximately 60–90 minutes. Furthermore, OES–ICP analysis detected a residual magnesium concentration below 0.05 mg L^{-1}, confirming that MgO nanoparticles remained effectively immobilized during treatment while maintaining high clarification efficiency. These findings demonstrate that the superior performance of the PPW–MgO nanocomposites is governed by the synergistic interaction of adsorption, charge neutralization, polymer bridging, and sweep flocculation, all of which are strongly influenced by MgO loading and solution pH.

4. CONCLUSION

The present study demonstrates an environmentally sustainable and scalable strategy for converting pomegranate peel waste into performance MgO-based nanocomposites for water purification. Among the synthesized formulations, PPW–MgO (0.50) exhibited the highest turbidity elimination efficiency (81.9%) under optimized operating conditions, owing to the combined effects of adsorption, polymer bridging, charge neutralization, and sweep flocculation. The excellent clarification efficiency, low residual magnesium concentration (<0.05 mg L^{-1}), and economical production cost demonstrate the potential of the developed material as a sustainable modification to conventional chemical coagulants. The current investigation employed synthetic kaolin suspensions to systematically evaluate the coagulation mechanism, future studies will focus on applying the optimized PPW–MgO nanocomposite to real textile wastewater and natural surface water for comprehensive assessment of COD, color, and microbial removal. Thus, the PPW–MgO nanocomposite provides a promising, environmentally friendly, and circular-economy-based material for advanced water and wastewater treatment applications.

FUNDING

This research received no specific grant from any funding agency in the public, commercial, or not-for-profit sectors.

CONFLICTS OF INTEREST

The authors declare that there is no conflict of interest.

COPYRIGHT

This article is an open-access article distributed under the terms and conditions of the Creative Commons Attribution (CC BY) license (http://creativecommons.org/licenses/by/4.0/).

REFERENCES

Abel, S. K., Amirtharajan, S., Mahalingam, A., Baskaran, S. and Pandurengan, S., Green synthesis of rGO/MgO nanocomposite using Hylocereus polyrhizus peel extract for antibacterial activity and photocatalytic dye degradation study, *Chem. Phys. Impact*, 10, 100885 (2025). https://doi.org/10.1016/j.chphi.2025.100885

Abinaya, N., Sivaranjana, P., Rajini, N. and Krishnan, K., Performance analysis of biodegradable composite using polyvinyl alcohol and pomegranate peel powder for sustainable dry packaging applications, *Discov. Mater.*, 4(1), 63 (2024). https://doi.org/10.1007/s43939-024-00139-w

Ahmed, H. M., El-Khateeb, M. A., Mohamed, N. Y., Sobhy, N. A. and Fawzy, M. E., Evaluation of different natural waste materials as bio-coagulants for domestic wastewater treatment, *Desalin. Water Treat.*, 317, 100034 (2024). https://doi.org/10.1016/j.dwt.2024.100034

Akmese, B., Removal of Brilliant Blue R and Victoria Blue R dyes from textile wastewater by adsorption method using pomegranate peel, *BMC Chem.*, 19(1), 99 (2025). https://doi.org/10.1186/s13065-025-01476-4

Al-Baidhani, J. H. and Al-Khafaji, A. H. J., Using of coagulation process of pomegranate peels for the tertiary treatment of wastewater, *Int. J. Appl. Eng. Res.*, 12(24), 14858–14864 (2017).

Al-Hussainy, A. F., Al-Saedi, H. F. S., Hanoon, H. N., Jasem, N. M., Hussein, M. A., Shaheen, B. S., Saadi, B. M. and Mueen, H., Utilization of agro-waste derived activated carbon for wastewater treatment: Adsorptive removal of brilliant blue dye, *Appl. Chem. Eng.*, 8(3), (2025). https://doi.org/10.59429/ace.v8i3.5721

Arif, S., Javaid, I., Israr, Z., Gillani, S. S. A. and Anwar, M. S., Sunlight-driven degradation of water pollutants using pomegranate-synthesized CuO nanoparticles, *Mater. Sci. Eng. B*, 310, 117749 (2024). https://doi.org/10.1016/j.mseb.2024.117749

Arif, S., Nawaz, M., Siddique, S., Ayub, R. and Saleem, S., Synthesis, characterization and photocatalytic activity of Mg1−xCuxO nanoparticles for wastewater treatment, *Mater. Today Commun.*, 33, 104361 (2022). https://doi.org/10.1016/j.mtcomm.2022.104361

Azizi, M. and Alorabi, A. Q., One-pot synthesis of kaolinite–modified pomegranate hydrochar composite for enhanced malachite green removal, *J. Environ. Chem. Eng.*, 13(6), 119379 (2025). https://doi.org/10.1016/j.jece.2025.119379

Bashyal, N., Aryal, S., Rai, R., Lohani, P. C., Gautam, S. K., Pokhrel, M. R. and Poudel, B. R., Effective Biosorption of Phosphate from Water Using Fe(III)-Loaded Pomegranate Peel, *Chem. Biochem. Eng. Q.*, 37(2), 67–77 (2023). https://doi.org/10.15255/CABEQ.2022.2174

Benahdach, K., Aoulad El Hadj Ali, Y., Azzouz, A., Mar Cerrillo, G. M. D., Chraka, A., Mail, R. E., Laghdach, A. E., Wahby, A. and Arhoun, B., Synthesis of activated carbon by microwave-assisted sulfuric acid activation for the adsorption of Congo Red in aqueous medium: Kinetic, isotherm, thermodynamic, molecular dynamic, and functional theory studies, *J. Mol. Liq.*, 420, 126821 (2025). https://doi.org/10.1016/j.molliq.2024.126821

Bodor, A., Bellahsen, N., Perei, K., Hodúr, C. and Feigl, G., Phytotoxicity evaluation of nutrient-fortified pomegranate peel powders prepared from food waste and their feasibility as biofertilizers, *Environ., Dev. Sustainable*, 26(2), 3671–3685 (2024). https://doi.org/10.1007/s10668-022-02852-z

David, D. M., Susan, P. V., Mahima, H. and Ram, K. S., Innovative Approaches in Nanomaterials for Efficient Heavy Metal Removal from Wastewater: A Scientific Review, *J. Environ. Nanotechnol.*, 13(4), 518-526 (2024). https://doi.org/10.13074/jent.2024.12.2441022

Fadhil, D. H., Al-Mashhadani, M. H., Mortada, W. I., Alsayed, R. and Khalifa, M. E., Eco-derived chitosan–cellulose hybrid from pomegranate peel for enhanced uptake of methyl orange dye, *Res. Chem.*, 27, 103371 (2026). https://doi.org/10.1016/j.rechem.2026.103371

Gaharwar, S. S., Majumdar, A. and Kumar, A., Pomegranate peel-derived activated carbon: An effective adsorbent for protocatechuic acid removal and environmental remediation, *Adsorption*, 30(8), 2219–2233 (2024). https://doi.org/10.1007/s10450-024-00550-y

Hamad, M. T. M. H. and Ibrahim, S., Effective fabrication and characterization of eco-friendly nano particles composite for adsorption Cd (II) and Cu (II) ions from aqueous solutions using modelling studies, *Sci. Rep.*, 14(1), 11767 (2024). https://doi.org/10.1038/s41598-024-61050-1

Hassan, M. A., El-Ashaal, E. S., Oun, A. A. and Farghali, M. A., Pomegranate Peel/Reduced Graphene Oxide-Based Nanocomposite as a Promising Adsorbent for Lead and Methylene Blue Remediation, *Chem. Africa*, 8(9), 4693–4715 (2025). https://doi.org/10.1007/s42250-025-01406-w

Henini, G., Khurshid, H., Laidani, Y., Henini, S., Umoren, S. A., Suleiman, R. K. and Meliani, M. H., An investigation into equilibrium, Kinetics, and thermodynamics of yellow bemacid dye removal from Aqueous Solutions using pomegranate skin (PG) and Date Pedicels (DPd) as Green Adsorbents, *Adsorption*, 30(8), 2099–2112 (2024). https://doi.org/10.1007/s10450-024-00546-8

Jalali, K., Pajootan, E. and Bahrami, H., Elimination of hazardous Methylene Blue from contaminated solutions by electrochemically magnetized graphene oxide as a recyclable adsorbent, *Adv. Powder Technol.*, 30(10), 2352–2362 (2019). https://doi.org/10.1016/j.apt.2019.07.018

Kalidasan, K., Vidaarth, T. M. N., Surendhiran, S., Jagan, K. S. G., Karthik, S., Kaviarasu, G. and Dufossé, L., Synthesis of phytochemical-enriched MgO nanoparticles using Sonneratia ovata leaf extract for photocatalytic activity and inactivation of bacteria, *J. Environ. Manage.*, 411, 130159 (2026). https://doi.org/10.1016/j.jenvman.2026.130159

Kamalesh, R. and Saravanan, A., Sustainable ANN-driven modelling and characterisation of Rhodamine-B removal using ZIF-8 functionalised pomegranate peel waste adsorbent supporting clean water and sanitation initiatives, *Hybrid Adv.*, 12, 100625 (2026). https://doi.org/10.1016/j.hybadv.2026.100625

Kumar, A., Poornima, S. N., Subbulakshmi, R., Selvaraju, M., G, R. K. and Jayabalan, C., Hierarchical green carbon fibers from banana pseudostem for efficient Pb^{2+} adsorption: Kinetics, isotherms, and machine learning prediction, *Interact.*, 247(1), 188 (2026). https://doi.org/10.1007/s10751-026-02534-6

Mahdy, A. and Fathi, N., Comparative Performance of Bio-Derived Nanomaterials for Chromium Removal from Contaminated Water, *Water Environ. Res.*, 98(4), e70382 (2026). https://doi.org/10.1002/wer.70382

Murat, D., Teğin, İ. and Saka, C., Optimization of nitrogen doping via microwave irradiation for improved adsorptive performance of pomegranate peel-derived biochar, *Chem. Eng. Res. Des.*, 220, 566–576 (2025). https://doi.org/10.1016/j.cherd.2025.07.040

Pachiyappan, J., Gnanansundaram, N., Sivamani, S., Sankari, N. P. B. P., Senthilnathan, N. and Kerga, G. A., Preparation and Characterization of Magnesium Oxide Nanoparticles and Its Application for Photocatalytic Removal of Rhodamine B and Methylene Blue Dyes, *J. Nanomater.*, 2022(1), 6484573 (2022). https://doi.org/10.1155/2022/6484573

Raj, C. K., Siranjeevi, R., Susmitha, R., Shabnum, S. S., Nivetha, P., Benazir, K., Saravanan, A. and Vickram, A. S., Evaluation of chitosan/diosgenin-infused manganese dioxide nanocomposite for highly effective photocatalytic and antibacterial activity, *Int. J. Biol. Macromol.*, 292, 139380 (2025). https://doi.org/10.1016/j.ijbiomac.2024.139380

Rao, D. P., Krishnasamy, V. D., Selvaraju, M., Sundramurthy, V. P., Kandavalli, S. R., Chitra, M. S., Sivasamy, N. and Thirumoorthy, P., Adsorptive removal of cadmium from electroplating wastewater using hybrid composite of thiol-grafted seed gum of Tamarindus indica and Teff hay biocarbon, *Zeitschrift Fur Physikalische Chemie*, 239(5), 633–654 (2025). https://doi.org/10.1515/zpch-2024-0715

Rashtbari, Y., Sher, F., Afshin, S., Hamzezadeh bahrami, A., Ahmadi, S., Azhar, O., Rastegar, A., Ghosh, S. and Poureshgh, Y., Green synthesis of zero-valent iron nanoparticles and loading effect on activated carbon for furfural adsorption, *Chemosphere*, 287, 132114 (2022). https://doi.org/10.1016/j.chemosphere.2021.132114

Shabanizadeh, H. and Taghavijeloudar, M., A sustainable approach for industrial wastewater treatment using pomegranate seeds in flocculation-coagulation process: Optimization of COD and turbidity removal by response surface methodology (RSM), *J. Water Process Eng.*, 53, 103651 (2023a). https://doi.org/10.1016/j.jwpe.2023.103651

Shabanizadeh, H. and Taghavijeloudar, M., Potential of pomegranate seed powder as a novel natural flocculant for pulp and paper wastewater treatment: Characterization, comparison and combination with alum, *Process Safety Environ. Protect.*, 170, 1217–1227 (2023b). https://doi.org/10.1016/j.psep.2023.01.004

Tamam, N., Mahadadalkar, M. A., Aadil, M., El-Aassar, M. R., Rafea, M. A., Zaki, M. E. A., Park, N., Elhadi, M. and Ahmad, Z., Unveiling the visible-light-driven photocatalytic aptitude of nanostructured MgO semiconductor synthesized using lemon peel extract, *Ceram. Int.*, 51(18), 25487–25498 (2025). https://doi.org/10.1016/j.ceramint.2025.03.231

Tom, A. P., Sustainable Technological Advancements for Dairy Wastewater Treatment-A Review, *J. Sol. Waste Technol. Manage.*, 49(3), 292–304 (2023). https://doi.org/10.5276/JSWTM/ISWMAW/492/2023.292

Zareei, J., Juraev, N., Hassan Widatalla, S. T., Kerwad, M., Olegovich Bokov, D., Alkhuzai, K. A., Rodriguez-Benites, C., Alhadrawi, M. and Zain Al-Abdeen, S. H., Investigation of the potential of pomegranate peel as a treatment option for heavy metal contaminated wastewater: Experimental and modeling approaches, *Heliyon*, 10(14), e34619 (2024). https://doi.org/10.1016/j.heliyon.2024.e34619